

# Efficient Algorithms for Bend-minimum Orthogonal Drawings of Planar 3-Graphs

Walter Didimo\*, Giuseppe Liotta\*, Maurizio Patrignani†

December 14, 2024

## Abstract

Let  $G$  be a planar 3-graph (i.e., a planar graph with vertex degree at most three) with  $n$  vertices. We prove that a planar orthogonal drawing of  $G$  with the minimum number of bends can be computed in  $O(n^2)$  time. The minimum is taken over all planar embeddings of  $G$ . The most efficient known algorithm to solve this problem has complexity  $\tilde{O}(n^{17})$ , as proved by Chang and Yen for biconnected planar 3-graphs [SoCG Proc., 2017]. If either a distinguished edge or a distinguished vertex of  $G$  is constrained to be on the external face, a bend-minimum orthogonal drawing of  $G$  that respects the given constraint can be computed in  $O(n)$  time. An additional feature of our algorithms is that they compute drawings with at most two bends per edge, which is worst-case optimal.

## 1 Introduction

An orthogonal drawing of a graph maps each vertex to a distinct point in the plane and represents each edge as a chain of horizontal and vertical segments (see Fig. 1). Orthogonal drawings find applications, for example, in information systems where they are the standard visualization paradigm for conceptual schemata and in VLSI design where circuital connections are typically wired by using vertical and horizontal tracks. See, e.g., [7, 9, 11, 17, 18, 20] for book chapters and surveys about orthogonal graph drawings and their applications.

Partly motivated by these applications and partly for the combinatorial beauty of the optimization problems, several algorithms have been designed to compute orthogonal drawings where readability parameters such as area, number of bends per edge, total number of bends, and total edge length are minimized. Dating back to 1980, a pioneering paper by Storer [24] initiates the study of these optimization goals and asks whether a crossing-free orthogonal drawing with the minimum number of bends can be computed in polynomial time. The question posed by Storer is in the fixed embedding setting, i.e., the input is a plane 4-graph (an embedded planar graph with vertex degree at most four) and the wanted output is an embedding-preserving orthogonal drawing with the minimum number of bends. Tamassia [25] solves Storer’s problem by describing an  $O(n^2 \log n)$ -time algorithm. The key idea of Tamassia’s result is the equivalence between the bend minimization problem and the problem of computing a min-cost flow on a suitable network. To date, the most efficient known solution of the bend-minimization problem for orthogonal drawings in the fixed embedding setting is due to Cornelsen and Karrenbauer [6], who show a novel technique to compute a min-cost flow on an uncapacitated network and apply this technique to Tamassia’s model achieving  $O(n^{\frac{3}{2}})$  time complexity.

A different level of complexity for the bend minimization problem is encountered in the variable embedding setting, that is when the algorithm is asked to find a bend-minimum solution over all planar embeddings of the graph. For example, the orthogonal drawing of Fig. 1c has a different planar embedding than the graph of Fig. 1a and it has no bends, while the drawing of Fig. 1b preserves the embedding but it is suboptimal in terms of bends.

---

\*Università degli Studi di Perugia, Italy [walter.didimo@unipg.it](mailto:walter.didimo@unipg.it)

†Università Roma Tre, Italy [patrigna@dia.uniroma3.it](mailto:patrigna@dia.uniroma3.it)

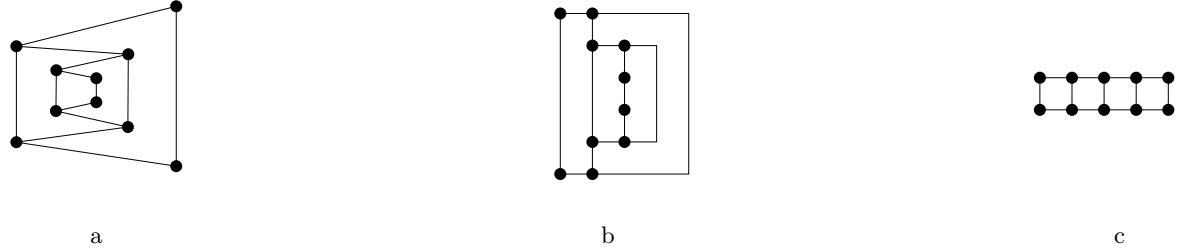


Figure 1: (a) A planar embedded 3-graph  $G$ . (b) An embedding-preserving bend-minimum orthogonal drawing of  $G$ . (c) A bend-minimum orthogonal drawing of  $G$ .

Garg and Tamassia [13] prove that the bend-minimization problem for orthogonal drawings is NP-complete for planar 4-graphs, while Di Battista et al. [8] show that it can be solved in  $O(n^5 \log n)$ -time for planar 3-graphs. Generalizations of the problem in the variable embedding setting where edges have some flexibility (i.e., they can bend a few times without cost for the optimization function) have also been the subject of recent studies [2].

Improving the  $O(n^5 \log n)$  time complexity of the algorithm by Di Battista et al. [8] has been an elusive open problem for more than a decade (see, e.g., [3]), until a recent paper by Chang and Yen [4] at SoCG 2017 has shown how to compute a bend-minimum orthogonal drawing of a planar 3-graph in the variable embedding setting in  $\tilde{O}(n^{17})$ -time<sup>1</sup>. Similar to [8], the approach in [4] uses an SPQR-tree to explore all planar embeddings of a planar 3-graph and combines partial solutions associated with the nodes of this tree to compute a bend-minimum drawing. Both in [8] and in [4], the most computationally expensive tasks are computing min-cost flows on suitable variants of Tamassia’s network. However, Chang and Yen elegantly prove that a simplified version of the flow network where all edges have unit capacity can be adopted to solve the problem; this, together with a recent result [5] about min-cost flows on unit-capacity networks, yields the improved time complexity.

**Contribution and outline.** In this paper we study the problem of computing an orthogonal drawing of a planar 3-graph in the variable embedding setting and improve the time complexity of the state-of-the-art solution. We prove the following.

**Theorem 1.** *Let  $G$  be an  $n$ -vertex planar 3-graph. A bend-minimum orthogonal drawing of  $G$  can be computed in  $O(n^2)$ -time. If either a distinguished edge or a distinguished vertex of  $G$  is constrained to be on the external face, a bend-minimum orthogonal drawing of  $G$  that respects the given constraint can be computed in  $O(n)$  time. Also, the computed drawings have at most two bends per edge, which is worst-case optimal.*

Similar to [8] and to [4], the algorithmic approach of Theorem 1 computes a bend-minimum orthogonal drawing by visiting an SPQR-tree of the input graph. However, it does not need to compute min-cost flows at any steps of the visit, which is the fundamental difference with the previous techniques. This makes it possible to design the first quadratic-time algorithm to compute bend-minimum orthogonal drawings of planar 3-graphs in the variable embedding setting. The second part of the statement of Theorem 1 extends previous studies by Nishizeki and Zhou [29], who give a first example of linear-time algorithm in the variable embedding setting for planar 3-graphs that are partial two-trees. Finally, the bend-minimum drawings of Theorem 1 have at most two bends per edge, which is a desirable property for an orthogonal representation. We recall that every planar 4-graph (except the octahedron) admits an orthogonal drawing with at most two bends per edge [1, 19]; however, minimizing the number of bends may require some edges with a  $\Omega(n)$  bends [8, 26].

The paper is organized as follows. Preliminary definitions and results are in Section 2. In Section 3 we prove key properties of bend-minimum orthogonal drawings of planar 3-graphs used in our approach. Section 4 describes our drawing algorithms. Conclusions and open problems are in Section 5.

<sup>1</sup>The  $\tilde{O}(\cdot)$  notation suppresses  $O(\log^k n)$  multiplicative factors, for some positive constant  $k$ .

## 2 Preliminaries

A graph  $G$  is *1-connected*, or *simply-connected*, if there is a path between any two vertices.  $G$  is  *$k$ -connected*, for  $k \geq 2$ , if the removal of  $k-1$  vertices leaves the graph 1-connected. A 2-connected (3-connected) graph is also called *biconnected* (*triconnected*).

For a graph  $G$ ,  $V(G)$  and  $E(G)$  denote the sets of vertices and edges of  $G$ . If not otherwise specified, we consider *simple* graphs, i.e., graphs with neither self-loops nor multiple edges. The *degree* of a vertex  $v \in V(G)$ , denoted as  $\deg(v)$ , is the number of its neighbors.  $\Delta(G)$  denotes the maximum degree of a vertex of  $G$ ; if  $\Delta(G) \leq h$  ( $h \geq 1$ ),  $G$  is an  *$h$ -graph*.

A *planar drawing* of  $G$  is a geometric representation in the plane such that: (i) each vertex  $v \in V(G)$  is drawn as a distinct point  $p_v$ ; (ii) each edge  $e = (u, v) \in E(G)$  is drawn as a simple curve connecting  $p_u$  and  $p_v$ ; (iii) no two edges intersect in  $\Gamma$  except at their common end-vertices (if they are adjacent). A graph is *planar* if it admits a planar drawing. A planar drawing  $\Gamma$  of  $G$  divides the plane into topologically connected regions, called *faces*. The *external face* of  $\Gamma$  is the region of unbounded size; the other faces are *internal*. A *planar embedding* of  $G$  is an equivalence class of planar drawings that define the same set of (internal and external) faces, and it can be described by the clockwise sequence of vertices and edges on the boundary of each face plus the choice of the external face. Graph  $G$  together a given planar embedding is an *embedded planar graph*, or simply a *plane graph*: If  $\Gamma$  is a planar drawing of  $G$  whose set of faces is that described by the planar embedding of  $G$ , we say that  $\Gamma$  *preserves* this embedding, or also that  $\Gamma$  is an *embedding-preserving drawing* of  $G$ .

A graph  $G$  is *rectilinear planar* if it admits a planar drawing where each edge is either a horizontal or a vertical segment (i.e., an orthogonal drawing without bends). Rectilinear planarity testing is NP-complete for planar 4-graphs [13], but it is polynomially solvable for planar 3-graphs [4, 8]. By extending a result of Thomassen [27] on those 3-graphs that have a rectilinear drawing with all rectangular faces, Rahman and Nishizeki [23] characterize rectilinear plane 3-graphs. For a plane graph  $G$ , let  $C_o(G)$  be its external cycle ( $C_o(G)$  is simple if  $G$  is biconnected). Also, if  $C$  is a simple cycle of  $G$ , denote by  $G(C)$  the plane subgraph of  $G$  that consists of  $C$  and of the vertices and edges inside  $C$ . An edge  $e = (u, v) \notin E(G(C))$  is a *leg* of  $C$  if exactly one of the vertices  $u$  and  $v$  belongs to  $C$ ; such a vertex is a *leg-vertex* of  $C$ . If  $C$  has exactly  $k$  legs in  $G$  and no edge outside  $C$  joins two its vertices,  $C$  is a  *$k$ -legged cycle* of  $G$ .

**Theorem 2.** [23] *Let  $G$  be a biconnected plane 3-graph.  $G$  admits an orthogonal drawing without bends if and only if: (i)  $C_o(G)$  contains at least four vertices of degree two; (ii) each 2-legged cycle contains at least two vertices of degree two; (iii) each 3-legged cycle contains at least one vertex of degree two.*

With the same terminology as in [23], we call *bad* any 2-legged and any 3-legged cycle that does not satisfy Condition (ii) and (iii) of Theorem 2, respectively.

**SPQR-trees of Planar 3-Graphs.** Let  $G$  be a biconnected graph. An *SPQR-tree*  $T$  of  $G$  represents the decomposition of  $G$  into its triconnected components and can be computed in linear time [7, 15, 16]. Each triconnected component of  $G$  is associated with a node  $\mu$  of  $T$ . The triconnected component itself is called the *skeleton* of  $\mu$ , and denoted as  $\text{skel}(\mu)$ . A node  $\mu$  of  $T$  can be of four different types: (i) *R-node*, if  $\text{skel}(\mu)$  is a triconnected graph; (ii) *S-node*, if  $\text{skel}(\mu)$  is a simple cycle of length at least three; (iii) *P-node*, if  $\text{skel}(\mu)$  is a bundle of at least three parallel edges; (iv) *Q-nodes*, if it is a leaf of  $T$ ; in this case the node represents a single edge of the graph and its skeleton consists of two parallel edges. Note that, neither two *S*- nor two *P*-nodes are adjacent in  $T$ . A *virtual edge* in  $\text{skel}(\mu)$  corresponds to a tree node  $\nu$  that is adjacent to  $\mu$  in  $T$ . If we assume that  $T$  is rooted at one of its *Q-nodes*  $\rho$ , then every skeleton (except the one of  $\rho$ ) contains exactly one virtual edge that has a counterpart in the skeleton of its parent: This virtual edge is called the *reference edge* of  $\text{skel}(\mu)$  and of  $\mu$ , and its endpoints are the *poles* of  $\text{skel}(\mu)$  and of  $\mu$ . The edge of  $G$  corresponding to the root  $\rho$  of  $T$  is the *reference edge* of  $G$ , and  $T$  is the SPQR-tree of  $G$  with respect to  $e$ . For every node  $\mu \neq \rho$  of  $T$ , the subtree  $T_\mu$  rooted at  $\mu$  induces a subgraph  $G_\mu$  of  $G$  called the *pertinent graph* of  $\mu$ , which is described by  $T_\mu$  in the decomposition: The edges of  $G_\mu$  are the edges of  $G$  corresponding to the *Q-nodes* (leaves) of  $T_\mu$ . Graph  $G_\mu$  is also called a *component* of  $G$  with respect to the reference edge  $e$ , namely  $G_\mu$  is a *P*-, an *R*-, or an *S*-component depending on whether  $\mu$  is a *P*-, an *R*-, or an *S*-component, respectively.

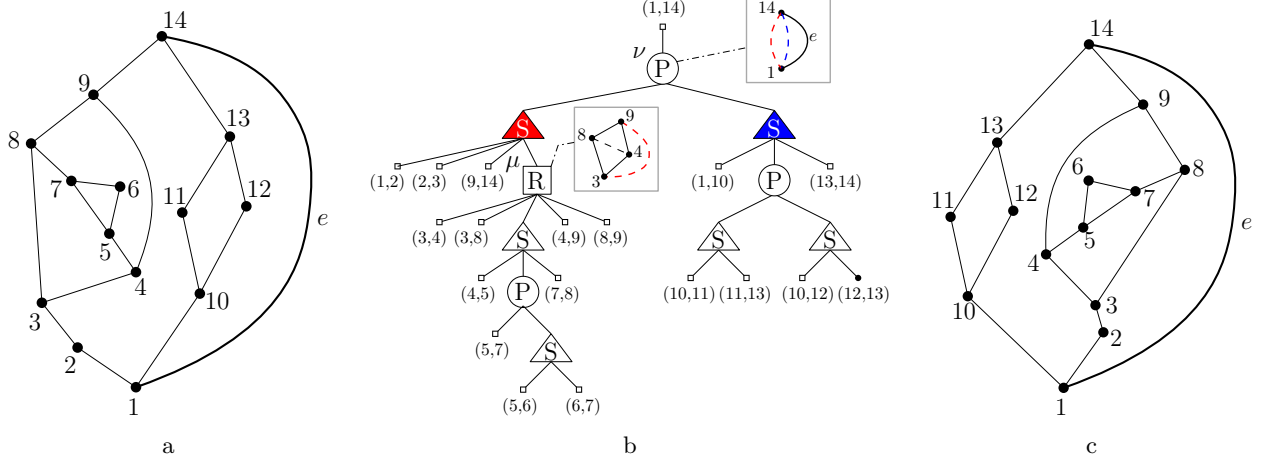


Figure 2: (a) A plane 3-graph  $G$ . (b) The SPQR-tree of  $G$  with respect to  $e$ . (c) A different embedding of  $G$  obtained by changing the embedding of  $\text{skel}(\nu)$  and of  $\text{skel}(\mu)$ .

The SPQR-tree  $T$  rooted at a Q-node  $\rho$  implicitly describes all planar embeddings of  $G$  having the reference edge of  $G$  on the external face. All such embeddings can be obtained by combining the different planar embeddings of the skeletons of P- and R-nodes: If  $\mu$  is a P-node, the different embeddings of  $\text{skel}(\mu)$  are obtained by the different permutations of its non-reference edges. If  $\mu$  is an R-node,  $\text{skel}(\mu)$  has two possible planar embeddings, obtained by flipping  $\text{skel}(\mu)$  minus its reference edge at its poles. Figure 2a shows a plane graph  $G$  with a reference edge  $e$ ; the SPQR-tree  $T$  of  $G$  with respect to  $e$  is in Fig. 2b; the skeletons of a P-node  $\nu$  and of the R-node  $\mu$  are shown, with a planar embedding consistent with that of  $G$ . Figure 2c depicts a different planar embedding of  $G$  with  $e$  on the external face, obtained by changing the embeddings of both  $\text{skel}(\mu)$  and  $\text{skel}(\nu)$ .

The child node  $\mu$  of  $\rho$  is called the *root child* of  $T$  and  $G_\mu$  is the *root child component*. An *inner node* is neither the root nor the root child of  $T$ . The pertinent graph of an inner node is an *inner component* of  $G$ . The next lemma gives basic properties of  $T$  when  $\Delta(G) \leq 3$ .

**Lemma 1.** *Let  $G$  be a biconnected planar 3-graph and let  $T$  be the SPQR-tree of  $G$  with respect to a reference edge  $e$ . Then:*

- T1** *Each P-node has exactly two children, one of them is an S-node and the other is either an S-node or a Q-node; if the P-node is the root child, both its children are S-nodes.*
- T2** *Each child of an R-node is either an S-node or a Q-node.*
- T3** *For each inner S-node  $\mu$ , the edges of  $\text{skel}(\mu)$  incident to the poles of  $\mu$  are (real) edges of  $G$ . Also, there cannot be two incident virtual edges in  $\text{skel}(\mu)$ .*

*Proof.* We prove the four properties separately.

- Proof of T1. By definition, a P-node  $\mu$  has at least two children. Also, since  $G$  has no multiple edges,  $\mu$  has at most one child that is a Q-node. At the same time, since  $\Delta(G) \leq 3$ ,  $\mu$  has neither three children nor a child that is an R-node, as otherwise at least one of its poles would have degree greater than 3 in  $G$ . Finally, if  $\mu$  is the root child of  $T$ , its poles coincide with the end-vertices of the reference edge  $e$ ; if a child of  $\mu$  is a Q-node,  $G$  has multiple edges, a contradiction.
- Proof of T2. Let  $\mu$  be a child of an R-node; if  $\mu$  is a P-node or an R-node, the poles of  $\mu$  have degree greater than one in  $G_\mu$ , which implies that these vertices have degree greater than three in  $G$ , a contradiction.

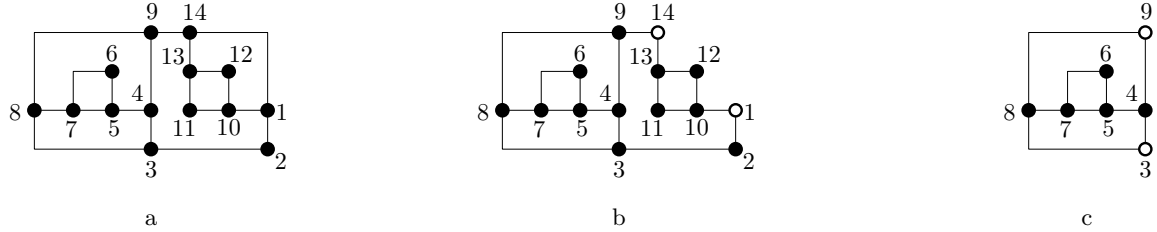


Figure 3: (a) A bend-minimum orthogonal representation  $H$  of the graph in Fig. 2a (the representation has four bends). (b) The component  $H_v$ , which is L-shaped; the two poles of the component are the white vertices. (c) The component  $H_\mu$ , which is D-shaped.

- Proof of T3. Let  $\mu$  be an inner S-node of  $T$  and let  $w$  be a pole of  $\mu$ . The parent of  $\mu$  in  $T$  is either a P-node or an R-node. If it is a P-node, then the edge incident to  $w$  in  $\text{skel}(\mu)$  cannot be a virtual edge, as otherwise  $w$  has degree at least two in  $G_\mu$  and it has at least two edges outside  $G_\mu$ ; this would contradict the fact that  $\Delta(G) \leq 3$ . If the parent node of  $\mu$  is an R-node, then  $w$  has exactly three incident edges in the skeleton of this R-node, thus it must have degree one in  $G_\mu$ . Finally, two virtual edges cannot be incident in  $\text{skel}(\mu)$ , as they would imply a vertex of degree four in the graph.

□

### 3 Properties of Bend-Minimum Orthogonal Representations of Planar 3-Graphs

We prove relevant properties of bend-minimum orthogonal drawings of planar 3-graphs that are independent of vertex and bend coordinates, but only depend on the vertex angles and edge bends. To this aim, we recall the concept of *orthogonal representation* [25] and define some types of “shapes” that we use to construct bend-minimum orthogonal representations.

**Orthogonal Representations.** Let  $G$  be a plane 3-graph. If  $v \in V(G)$  and if  $e_1$  and  $e_2$  are two (possibly coincident) edges incident to  $v$  that are consecutive in the clockwise order around  $v$ , we say that  $a = \langle e_1, v, e_2 \rangle$  is an *angle at  $v$  of  $G$*  or simply an *angle of  $G$* . Let  $\Gamma$  and  $\Gamma'$  be two orthogonal drawings of  $G$  that preserve its planar embedding. We say that  $\Gamma$  and  $\Gamma'$  are *equivalent* if: (i) For any angle  $a$  of  $G$ , the geometric angle corresponding to  $a$  is the same in  $\Gamma$  and  $\Gamma'$ , and (ii) for any edge  $e = (u, v)$  of  $G$ , the sequence of left and right bends along  $e$  moving from  $u$  to  $v$  is the same in  $\Gamma$  and in  $\Gamma'$ . An *orthogonal representation*  $H$  of  $G$  is a class of equivalent orthogonal drawings of  $G$ ;  $H$  can be described by the embedding of  $G$  together with the geometric value of each angle of  $G$  (90, 180, 270 degrees)<sup>2</sup> and with the sequence of left and right turns along each edge. Figure 3a shows a bend-minimum orthogonal representation of the graph in Fig. 2a.

Let  $p$  be a path from two vertices  $u$  and  $v$  in  $H$ . The *turn number* of  $p$  is the absolute value of the difference between the number of right and the number of left turns encountered along  $p$  moving from  $u$  to  $v$  (or vice versa). The turn number of  $p$  is denoted by  $t(p)$ . Note that, a turn along  $p$  is caused either by a bend on an edge of  $p$  or by an angle of 90 degrees (or equivalently of 270 degrees) at a vertex of  $p$ . For example, in the orthogonal representation of Fig. 3a, the turn number of the path  $\langle 3, 4, 5, 6, 7 \rangle$  is two.

We remark that if  $H$  is a bend-minimum orthogonal representation, the bends along an edge, while moving from an end-vertex to the other, are all left turns or all right turns. Indeed, if this is not the case, a left and a right turn can be removed from  $H$ , so obtaining an orthogonal representation with fewer bends than  $H$ , a contradiction (see, e.g., [25]).

**Shapes of Orthogonal Representations.** Let  $G$  be a biconnected planar 3-graph,  $T$  be the SPQR-tree of  $G$  with respect to a reference edge  $e \in E(G)$ , and  $H$  be an orthogonal representation of  $G$  with  $e$  on the

<sup>2</sup>Angles of 360 degrees only occurs at 1-degree vertices, thus one can avoid to specify them.

external face. For a node  $\mu$  of  $T$ , denote by  $H_\mu$  the restriction of  $H$  to a component  $G_\mu$ . We also call  $H_\mu$  a *component* of  $H$ . In particular,  $H_\mu$  is a P-, an R-, or an S-component depending on whether  $\mu$  is a P-, an R-, or an S-node, respectively. If  $\mu$  is the root child of  $T$ , then  $H_\mu$  is the *root child component* of  $H$ . Denote by  $u$  and  $v$  the two poles of  $\mu$  and let  $p_l$  and  $p_r$  be the two paths from  $u$  to  $v$  on the external boundary of  $H_\mu$ , one walking clockwise and the other walking counterclockwise on the external boundary. These paths are the *contour paths* of  $H_\mu$ . If  $\mu$  is an S-node,  $p_l$  and  $p_r$  share some edges (they even coincide if  $H_\mu$  is just a sequence of edges). If  $\mu$  is either a P- or an R-node,  $p_l$  and  $p_r$  are edge disjoint paths; in this case, we define the following *shapes* for  $H_\mu$ , depending on the values of  $t(p_l)$  and  $t(p_r)$ :

- $H_\mu$  is *C-shaped*, or -shaped, if  $t(p_l) = 2$  and  $t(p_r) = 4$ , or vice versa;
- $H_\mu$  is *D-shaped*, or -shaped, if  $t(p_l) = 0$  and  $t(p_r) = 2$ , or vice versa;
- $H_\mu$  is *L-shaped*, or -shaped, if  $t(p_l) = 1$  and  $t(p_r) = 3$ , or vice versa;
- $H_\mu$  is *X-shaped*, or -shaped, if  $t(p_l) = t(p_r) = 1$ .

For example, the component  $H_\nu$  in Fig. 3b is -shaped, while  $H_\mu$  in Fig. 3c is -shaped. Concerning S-components, the following lemma rephrases a result in [8, Lemma 4.1], and it is also an easy consequence of Property T3 in Lemma 1.

**Lemma 2.** *Let  $H_\mu$  be an inner S-component with poles  $u$  and  $v$  and let  $p_1$  and  $p_2$  be any two paths connecting  $u$  and  $v$  in  $H_\mu$ . Then  $t(p_1) = t(p_2)$ .*

Based on Lemma 2, we can describe the shape of an inner S-component  $H_\mu$  in terms of the turn number of any path  $p$  between its two poles: We say that  $H_\mu$  is a *k-spiral* if  $t(p) = k$ ; the value  $k$  is the *spirality* of  $H_\mu$ . The notion of spirality of an orthogonal component has been originally defined in [8]. Differently from [8], we restrict the definition of spirality to inner S-components and we always consider absolute values, instead of both positive and negative values depending on whether the left turns are more or fewer than the right turns. For instance, in the representation of Fig. 3a the two series with poles  $\{1, 14\}$  (the red and blue series of Fig. 2b) have spirality three and one, respectively; the series with poles  $\{4, 8\}$  (child of the R-node) has spirality zero, while the series with poles  $\{5, 7\}$  has spirality two.

We now give a key result that claims the existence of a bend-minimum orthogonal representation with specific properties for any biconnected planar 3-graph. This result will be used to design our drawing algorithm. Given an orthogonal representation  $H$ , we denote by  $\overline{H}$  the orthogonal representation obtained from  $H$  by replacing each bend with a dummy vertex:  $\overline{H}$  is called the *rectilinear image* of  $H$ ; a dummy vertex in  $\overline{H}$  is a *bend vertex*. Also, if  $w$  is a degree-2 vertex with neighbors  $u$  and  $v$ , *smoothing*  $w$  is the reverse operation of an edge subdivision, i.e., it replaces the two edges  $(u, w)$  and  $(w, v)$  with the single edge  $(u, v)$ .

**Lemma 3.** *Let  $G$  be a biconnected planar 3-graph with a given reference edge  $e$ .  $G$  admits a bend-minimum orthogonal representation  $H$  with  $e$  on the external face such that:*

- O1** *Every edge of  $H$  has at most two bends, which is worst-case optimal;*
- O2** *Every inner P-component or R-component of  $H$  is either -shaped or -shaped;*
- O3** *Every inner S-component of  $H$  has spirality at most four.*

*Proof.* We prove the existence of a bend-minimum orthogonal representation  $H$  that satisfies O1-O3 in three steps. We start by a bend-minimum orthogonal representation of  $G$  with  $e$  on the external face, and in the first step we prove that it either satisfies O1 or it can be locally modified, without changing its planar embedding, so to satisfy this property. In the second step, we prove that from the orthogonal representation obtained in the first step we can derive a new orthogonal representation (again with same embedding) that satisfies O2 in addition to O1. Finally, we prove that this last representation also satisfies O3.

**Step 1: Property O1.** Suppose that  $H$  is a bend-minimum orthogonal representation of  $G$  with  $e$  on the external face and having an edge  $g$  (possibly coincident with  $e$ ) with at least three bends. Let  $\overline{H}$  be the rectilinear image of  $H$ , and let  $\overline{G}$  be the plane graph underlying  $\overline{H}$ . Since  $\overline{H}$  has no bend,  $\overline{G}$  satisfies Conditions (i) – (iii) of Theorem 2. Denote by  $v_1, v_2$ , and  $v_3$  three bend vertices in  $\overline{H}$  that correspond to three

bends of  $g$  in  $H$ . Assume first that  $g$  is an internal edge of  $G$  (i.e.,  $g$  does not belong to the external face). Let  $\overline{G}'$  be the plane graph obtained from  $\overline{G}$  by smoothing  $v_1$ . We claim that  $\overline{G}'$  still satisfies Conditions (i) – (iii) of Theorem 2. Indeed, if this is not the case, there must be a bad cycle in  $\overline{G}'$  that contains both  $v_2$  and  $v_3$ . This is a contradiction, because no bad cycle can contain two vertices of degree two. It follows that there exists an (embedding-preserving) orthogonal representation  $\overline{H}'$  of  $\overline{G}'$  without bends, which is the rectilinear image of an orthogonal representation of  $G$  with fewer bends than  $H$ , a contradiction. Assume now that  $g$  is on the external cycle  $C_o(G)$  of  $G$ . If  $C_o(\overline{G})$  contains more than four vertices of degree two, then we can smooth vertex  $v_1$  and apply the same argument as above to contradict the optimality of  $H$  (note that, such a smoothing does not violate Condition (i) of Theorem 2). Suppose vice versa that  $C_o(\overline{G})$  contains exactly four vertices of degree two (three of them being  $v_1$ ,  $v_2$ , and  $v_3$ ). In this case, just smoothing  $v_1$  violates Condition (i) of Theorem 2. However, we can smooth  $v_1$  and subdivide an edge of  $C_o(\overline{G}) \cap C_o(G)$  (such an edge exists because  $C_o(G)$  has at least three edges and, by hypothesis and a simple counting argument, at least one of its edges has no bend in  $H$ ). The resulting plane graph  $\overline{G}''$  still satisfies the three conditions of Theorem 2 and admits a representation  $\overline{H}''$  without bends; the orthogonal representation of which  $\overline{H}''$  is the rectilinear image is a bend-minimum orthogonal representation of  $G$  with at most two bends per edge. To see that two bends per edge is worst case optimal, just consider the complete graph  $K_4$  on four vertices. Every planar embedding of  $K_4$  has three edges on  $C_o(K_4)$ . By Condition (i) of Theorem 2, a bend-minimum orthogonal representation of  $K_4$  has four bends on the external face and thus two of them are on the same edge.

**Step 2: Property O2.** Let  $H$  be a bend-minimum orthogonal representation of  $G$  that satisfies O1 and let  $\overline{H}$  be its rectilinear image. The plane underlying graph  $\overline{G}$  of  $\overline{H}$  satisfies the three conditions of Theorem 2. Rhaman, Nishizeki, and Naznin [23, Lemma 3] prove that, in this case,  $\overline{G}$  has an embedding-preserving orthogonal representation  $\overline{H}'$  without bends in which every 2-legged cycle  $C$  is either  $\square$ -shaped or  $\square$ -shaped, where the two poles of the shape are the two leg-vertices of  $C$ . On the other hand, if  $G_\mu$  is an inner P-component or an inner R-component, the external cycle  $C_o(G_\mu)$  is a 2-legged cycle of  $G$ , where the two leg-vertices of  $C_o(G_\mu)$  are the poles of  $G_\mu$ . Indeed,  $C_o(G_\mu)$  is a simple cycle and each pole has exactly one incident edge not belonging to  $G_\mu$ . It follows that, the orthogonal representation  $H'$  of  $G$  whose rectilinear image is  $\overline{H}'$  satisfies O2, as  $H'_\mu$  is either  $\square$ -shaped or  $\square$ -shaped. Also note that the bends of  $H'$  are the same as in  $H$ , because the bend vertices of  $\overline{H}$  coincide with those of  $\overline{H}'$ . Hence,  $H'$  still satisfies O1 and has the minimum number of bends.

**Step 3: Property O3.** Suppose now that  $H$  is a bend-minimum orthogonal representation of  $G$  (with  $e$  on the external face) that satisfies both O1 and O2. More precisely, assume that  $H \leftarrow H'$  is the orthogonal representation obtained in the previous step, where its rectilinear image  $\overline{H}$  is computed by the algorithm of Rhaman et al. [23], which we simply call **NoBend-Alg**. This algorithm works as follows (see also Fig. 4). In the first step, it arbitrarily designates four degree-2 vertices  $x, y, w, z$  on the external face. A 2-legged cycle (resp. 3-legged cycle) of the graph is *bad* with respect to these four vertices if it does not contain at least two (resp. one) of them; a bad cycle  $C$  is *maximal* if it is not contained in  $G(C')$  for any other bad cycle  $C'$ . The algorithm finds every maximal bad cycle  $C$  (the maximal bad cycles are independent of each other) and it collapses  $G(C)$  into a supernode  $v_C$ . Then it computes a rectangular representation  $R$  of the resulting coarser plane graph (i.e., a representation with all rectangular faces) where each of  $x, y, w, z$  (or a supernode containing it) is an external corner. Such a representation exists because the graph satisfies a characterization of Thomassen [27]. In the next steps, for each supernode  $v_C$ , **NoBend-Alg** recursively applies the same approach to compute an orthogonal representation of  $G(C)$ ; if  $C$  is 2-legged (resp. 3-legged), then two (resp. three) designated vertices coincide with the leg-vertices of  $C$ . The representation of each supernode is then “plugged” into  $R$ .

Suppose now that  $H_\mu$  is an inner S-component of  $H$  and let  $u$  and  $v$  be its poles. Let  $B_1, \dots, B_h$  be the biconnected components of  $G_\mu$  that are not single edges. We call each  $B_i$  a *subcomponent* of  $G_\mu$  (if  $G_\mu$  is a sequence of edges, it has no subcomponents). Consider a generic step of **NoBend-Alg**, in which it has to draw  $G(C)$ , for some cycle  $C$  (possibly the external cycle of  $G$ ) such that  $G_\mu \subseteq G(C)$ . We distinguish between three cases.

Case 1.  $G_\mu$  is not contained in any maximal bad cycle. If all the edges of  $G_\mu$  are internal edges of  $G(C)$ , the

external cycle  $C_o(B_i)$  of each  $B_i$  is a maximal bad 2-legged cycle (as it contains no designated vertices). In this case each  $G(C_0(B_i))$  is collapsed into a supernode, and in the rectangular drawing  $R$  of the resulting graph all the degree-2 vertices and supernodes of the series will belong to the same side of a rectangular face. Thus, when all subcomponents of  $H_\mu$  are drawn and plugged into  $R$ ,  $H_\mu$  gets spirality zero. If  $G_\mu$  has some edges on the external face, then some  $C_o(B_i)$  might not be a maximal bad cycle (in which case it contains at least two designated vertices); in this case the spirality of  $H_\mu$  will be equal to the number of designated vertices on its external edges, which is at most four.

Case 2.  $G_\mu$  is contained in a maximal bad cycle  $C'$  that passes through both  $u$  and  $v$ . In this case,  $G(C')$  is collapsed into a supernode  $v_{C'}$  before the computation of a rectangular drawing  $R$ . The two legs of  $C'$  that are incident to  $u$  and  $v$  will form at  $v_{C'}$  in  $R$  either two flat angles or a right angle: In the former case,  $H_\mu$  will have spirality zero, while in the latter case it will have spirality one.

Case 3.  $G_\mu$  is contained in a maximal bad cycle  $C'$  that does not pass through both  $u$  and  $v$ . In this case,  $G(C')$  is still collapsed into a supernode  $v_{C'}$  before the computation of a rectangular drawing  $R$ , and in one of the subsequent steps of the recursive algorithm on  $G(C')$  we will fall in Case 1 or in Case 2.  $\square$

Figure 4 shows an example of how **NoBend-Alg** works. The input plane graph is in Fig. 4a, and it is the same graph  $G$  as Fig. 2a, with the addition of some degree-2 vertices (small squares), needed to satisfy the properties of Theorem 2. The external face of  $G$  contains exactly four degree-2 vertices, which are assumed to be the four designated vertices in the first step of **NoBend-Alg**. In the figure, the bad cycles with respect to the designated vertices are highlighted in red; the two cycles with thicker boundaries are maximal, and they are collapsed as shown in Fig. 4b. Note that, one of the two maximal cycles includes a designated vertex; once this cycle is collapsed, the corresponding supernode becomes the new designated vertex. Figure 4c depicts a rectangular representation of the graph in Fig. 4b, and it also shows the representations of the subgraphs in the supernodes, computed in the recursive procedure of **NoBend-Alg**; these representations are plugged in the rectangular representation, in place of the supernodes, yielding the final representation of Fig. 4d.

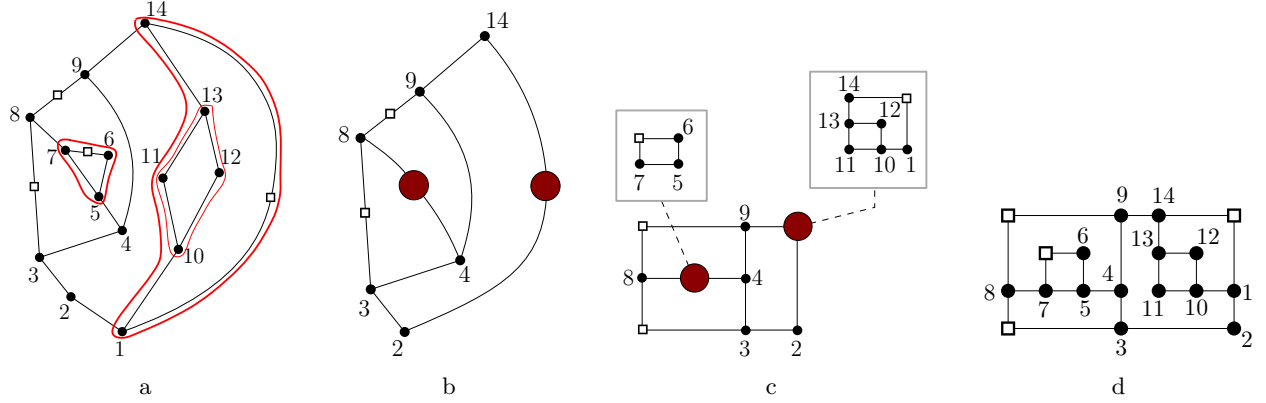


Figure 4: An illustration of the algorithm **NoBend-Alg**, described by Rahaman, Nishizeki, and Naznin [23].

## 4 Drawing Algorithm

Let  $G$  be a biconnected 3-planar graph  $G$  and let  $e$  be a distinguished edge of  $G$ . We first describe in Section 4.1 a linear-time algorithm to compute the bend-minimum orthogonal representations of the inner components of the SPQR-tree  $T$  of  $G$  with respect to  $e$ . In Section 4.2 we explain how to handle the root child of  $T$  to complete a bend-minimum orthogonal representation of  $G$  with  $e$  on the external face. Thanks to Lemma 3, our algorithm will search for a representation that satisfies Properties O1-O3. Section 4.3 describes how to extend our linear-time algorithm to simply-connected graphs.

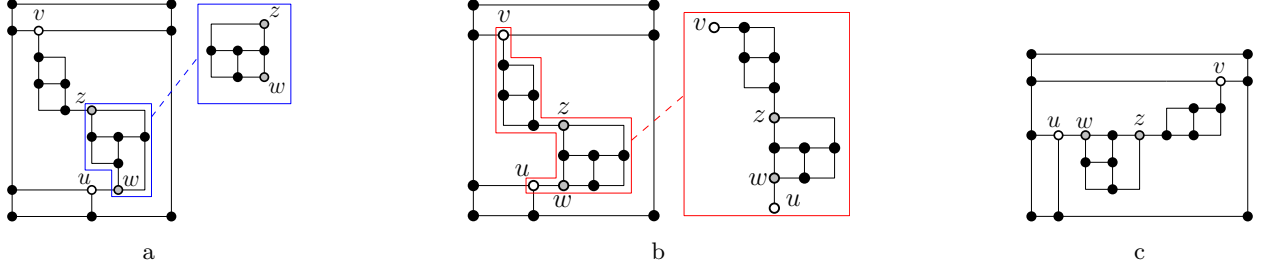


Figure 5: (a) An orthogonal representation  $H$ ; a D-shaped R-component with poles  $\{w, z\}$  and an equivalent representation of it are in the blue frames. (b) An orthogonal representation obtained from  $H$  by replacing the R-component with the equivalent one; a 1-spiral S-component with poles  $\{u, v\}$  and an equivalent representation are also shown in the red frames. (c) The orthogonal representation obtained by replacing the S-component with poles  $\{u, v\}$  with the equivalent one.

#### 4.1 Computing Orthogonal Representations for Inner Components

Let  $T$  be the SPQR-tree of  $G$  with respect to reference edge  $e$  and let  $\mu$  be an inner node of  $T$ . A key ingredient of our algorithm is the concept of ‘equivalence’ of orthogonal representations of  $G_\mu$ . Intuitively, two representations of  $G_\mu$  are equivalent if one can replace the other in any orthogonal representation of the whole graph. Similar equivalence concepts have been used for orthogonal drawings [8, 10]. As we shall prove (see Theorem 3), for planar 3-graphs a simplified definition of equivalent representations suffices. If  $\mu$  is a P-node or an R-node, two representations  $H_\mu$  and  $H'_\mu$  are *equivalent* if they are both  $\blacksquare$ -shaped or both  $\blacksquare$ -shaped. If  $\mu$  is an inner S-node,  $H_\mu$  and  $H'_\mu$  are *equivalent* if they have the same spirality.

**Lemma 4.** *If  $H_\mu$  and  $H'_\mu$  are two equivalent orthogonal representations of  $G_\mu$ , the two contour paths of  $H_\mu$  have the same turn number as the two contour paths of  $H'_\mu$ .*

*Proof.* The proof is trivial if  $\mu$  is a P-node or an R-node since, in order to be equivalent,  $H_\mu$  and  $H'_\mu$  must be both  $\blacksquare$ -shaped or  $\blacksquare$ -shaped, which, by definition, implies that their contour paths have the same turn numbers. If  $\mu$  is an S-node, then  $H_\mu$  and  $H'_\mu$  have the same spirality  $k$  and, by Lemma 2, their contour paths have the same turn number  $k$  as any path from one pole of  $\mu$  to the other pole.  $\square$

Suppose that  $H_\mu$  is an inner component of  $H$  with poles  $u$  and  $v$ , and let  $p_l$  and  $p_r$  be the contour paths of  $H_\mu$ . Replacing  $H_\mu$  in  $H$  with an equivalent representation  $H'_\mu$  means to insert  $H'_\mu$  in  $H$  in place of  $H_\mu$ , in such a way that: (i) if  $H_\mu$  and  $H'_\mu$  are  $\blacksquare$ -shaped, the contour path  $p'$  of  $H'_\mu$  for which  $t(p') = t(p_l)$  is traversed clockwise from  $u$  to  $v$  on the external boundary of  $H'_\mu$  (as for  $p_l$  on the external boundary of  $H_\mu$ ); (ii) in all cases, the external angles of  $H'_\mu$  at  $u$  and  $v$  are the same as in  $H_\mu$ . This operation may require to mirror  $H'_\mu$  (see Fig. 5). The next theorem uses arguments similar to [8].

**Theorem 3.** *Let  $H$  be an orthogonal representation of a planar 3-graph  $G$  and let  $H_\mu$  be the restriction of  $H$  to  $G_\mu$ , where  $\mu$  is an inner component of the SPQR-tree  $T$  of  $G$  with respect to a reference edge  $e$ . Replacing  $H_\mu$  in  $H$  with an equivalent orthogonal representation  $H'_\mu$  yields a planar orthogonal representation  $H'$  of  $G$ .*

*Proof.* The statement easily follows from Lemma 4 and from a characterization of orthogonal representations first stated in [28]. Let  $G$  be a biconnected embedded planar graph and let  $\phi$  be a function that assigns: (i) a value in  $\{90^\circ, 180^\circ, 270^\circ\}$  to each pair of consecutive edges in the circular order around each vertex  $v$  of  $G$  and (ii) a sequence of left and right turns to each edge  $e = (u, v)$  of  $G$ . Denote by  $t(f)$  the *turn number* of a face  $f$ , that is, the difference between the number of right and the number of left turns encountered while clockwise traversing the border of  $f$ , where a  $180^\circ$  angle counts as zero, a  $90^\circ$  angle (resp.,  $270^\circ$  angle) counts as one if  $f$  is an internal face (resp., if  $f$  is the external face), and a  $270^\circ$  angle (resp.,  $90^\circ$  angle) counts as  $-1$  if  $f$  is an internal face (resp., if  $f$  is the external face). Then  $\phi$  corresponds to an orthogonal representation  $H_\phi$  of  $G$  if and only if the turn number  $t(f)$  of each face  $f$  is four.

Hence, an orthogonal representation  $H$  of  $G$  induces an assignment  $\phi$  satisfying the above mentioned property. Let  $\phi_\mu$  be the restriction of  $\phi$  to the internal faces of  $H_\mu$ . Let  $H'_\mu$  be an orthogonal representation of  $G_\mu$  equivalent to  $H_\mu$  and let  $\phi'_\mu$  be the assignment corresponding to  $H'_\mu$ . We now prove that replacing  $H_\mu$  with  $H'_\mu$  yields a new orthogonal representation  $H'$  by showing that the corresponding function  $\phi'$  satisfies the above characterization. In the following, assuming that  $u$  and  $v$  are the two poles of  $H_\mu$  and that  $p_l$  and  $p_r$  are the two contour paths of  $H_\mu$ , we call  $p'_l$  the contour path of  $H'_\mu$  such that  $t(p'_l) = t(p_l)$  and  $p'_r$  the contour path of  $H'_\mu$  such that  $t(p'_r) = t(p_r)$  (if a mirroring of  $H'_\mu$  is needed in the replacement, the two contour paths of  $H'_\mu$  are renamed). Also, let  $f_l$  be the face of  $H$  to the left of  $p_l$  while moving along  $p_l$  from  $u$  to  $v$ , and let  $f'_l$  be the face of  $H'$  to the left of  $p'_l$  while moving along  $p'_l$  from  $u$  to  $v$ . The faces  $f_r$  and  $f'_r$  are defined symmetrically. Assignment  $\phi'$  is such that: (a) Each face  $f$  of  $H'$  whose boundary is exclusively composed of edges not belonging to  $G_\mu$  has the same shape as in  $H$  and for the angles and edges of  $f$  we have  $\phi' = \phi$ , hence  $t(f) = 4$ . (b) Each face  $f$  whose boundary is exclusively composed of edges of  $G_\mu$  has the same shape as in  $H'_\mu$  and for the angles and edges of  $f$  we have  $\phi' = \phi'_\mu$ , hence  $t(f) = 4$ . (c) The remaining two faces of  $H'$  are  $f'_l$  and  $f'_r$ . The boundary of  $f_l$  is composed of path  $p_l$  plus another path  $p$ . By construction, the boundary of  $f'_l$  is composed of path  $p'_l$  plus  $p$ . Also, again by construction, the two angles at  $u$  and  $v$  in  $f_l$  are the same as the two angles at  $u$  and  $v$  in  $f'_l$ . Since  $t(p_l) = t(p'_r)$  the turn number of  $f'_l$  in  $H'$  equals the turn number of  $f_l$  in  $H$ . The same for  $f'_r$ .  $\square$

We are now ready to describe our drawing algorithm. It is based on a dynamic programming technique, which visits bottom-up the SPQR-tree  $T$  with respect to the reference edge  $e$  of  $G$ . Based on Lemma 3 and Theorem 3, the algorithm stores for each visited node  $\mu$  of  $T$  a *set of candidate orthogonal representations* of  $G_\mu$ , together with their cost in terms of bends. Namely: (i) For a Q-node, the set of candidate orthogonal representations consists of three representations, with zero, one, and two bends, respectively. This suffices by Property O1 of Lemma 3. (ii) For a P-node or an R-node, the set of candidate orthogonal representations consists of a bend-minimum  $\blacksquare$ -shaped and a bend-minimum  $\blacksquare$ -shaped representation. This suffices by Property O2 of Lemma 3. (iii) For an S-node, the set of candidate orthogonal representations consists of a bend-minimum orthogonal representation for each value of spirality in  $\{0, 1, 2, 3, 4\}$ . This suffices by Property O3 of Lemma 3. We now describe how to compute the set of candidate representations for a node  $\mu$  that is a P-, an S-, or an R-node (computing the set of a Q-node is trivial). To achieve overall linear-time complexity, the candidate representations stored at  $\mu$  are described incrementally, linking the desired representation in the set of the children of  $\mu$  for each virtual edge of  $\text{skel}(\mu)$ .

**Candidate Representations for a P-node.** By property T1 of Lemma 1,  $\mu$  has two children  $\mu_1$  and  $\mu_2$ , where  $\mu_1$  is an S-node and  $\mu_2$  is an S-node or a Q-node. The cost of the  $\blacksquare$ -shaped representation of  $\mu$  is the sum of the costs of  $\mu_1$  and  $\mu_2$  both with spirality one. The cost of the  $\blacksquare$ -shaped representation of  $\mu$  is the minimum between the cost of  $\mu_1$  with spirality two and the cost of  $\mu_2$  with spirality two. This immediately implies the following.

**Lemma 5.** *Let  $\mu$  be an inner P-node. There exists an  $O(1)$ -time algorithm that computes a set of candidate orthogonal representations of  $G_\mu$  such that every element of the set has at most two bends per edge.*

**Candidate Representations for an S-node.** By property T3 of Lemma 1,  $\text{skel}(\mu)$ , without its reference edge, is a sequence of edges, such that the first edge and the last edge are real (i.e., they correspond to Q-nodes) and at most one virtual edge, corresponding to either a P-node or an R-node, may appear between two real edges. Let  $c_0$  be the sum of the costs of the cheapest (in terms of bends) orthogonal representations of all P-nodes and R-nodes corresponding to the virtual edges of  $\text{skel}(\mu)$ . By Property O2, each of these representations is either  $\blacksquare$ - or  $\blacksquare$ -shaped. Let  $n_Q$  be the number of edges of  $\text{skel}(\mu)$  that correspond to Q-nodes and let  $n_D$  be the number of edges of  $\text{skel}(\mu)$  that correspond to P- and R-nodes whose cheapest representation is  $\blacksquare$ -shaped. Obviously, any bend-minimum orthogonal representation of  $G_\mu$  satisfying O2 has cost at least  $c_0$ . We have the following.

**Lemma 6.** *An inner S-component admits an orthogonal representation with the minimum number of bends respecting Properties O1-O3 of Lemma 3 with cost  $c_0$  if its spirality  $k \leq n_Q + n_D - 1$  and with cost  $c_0 + k - n_Q - n_D + 1$  if  $k > n_Q + n_D - 1$ .*

*Proof.* The proof is by induction on the number of children of  $\mu$  that are not Q-nodes. Suppose that  $\mu$  has only Q-node children ( $n_D = 0$ ). It is trivial that  $G_\mu$ , which is a path, can be drawn with cost zero and with spirality in  $[0, \dots, n_Q - 1]$ , while has increasing costs for higher values of spirality. For the inductive case, note that inserting an  $\square$ -shaped child in between two Q-nodes does not increase nor decrease the spirality of an orthogonal drawing of  $G_\mu$ . Instead, a  $\square$ -shaped child inserted in between two Q-nodes can be used as if it were an additional Q-node to increase the spirality of one unit without additional costs.  $\square$

Observe that the possible presence in  $\text{skel}(\mu)$  of virtual edges corresponding to P-nodes and R-nodes whose cheapest representation is  $\square$ -shaped does not increase the spirality reachable at cost  $c_0$  by the S-node. Lemma 6 also provides an alternative proof of a known result ([8, Lemma 5.2]), stating that the minimum number of bends required by an orthogonal representation of an inner S-component in a planar 3-graph does not decrease when its spirality increases. Moreover, since for an inner S-component  $n_Q \geq 2$ , a consequence of Lemma 6 is the following.

**Corollary 1.** *For each  $k \in \{0, 1\}$ , every inner S-component admits a bend-minimum orthogonal representations of cost  $c_0$  with spirality  $k$ .*

Corollary 1 implies that every bend-minimum orthogonal drawing of an inner S-component with spirality at most one does not require additional bends with respect to the bend-minimum orthogonal drawings of their subcomponents.

**Lemma 7.** *Let  $\mu$  be an inner S-node and  $n_\mu$  be the number of vertices of  $\text{skel}(\mu)$ . There exists an  $O(n_\mu)$ -time algorithm that computes a set of candidate orthogonal representations of  $G_\mu$  such that every element of the set has at most two bends per edge.*

*Proof.* By virtue of Lemma 6 we can sum up the cheapest costs of the representations of all P- and R-node children of  $\mu$  to obtain the cost  $c_0$  of a bend-minimum orthogonal representation of  $\mu$  with spirality in  $[0, \dots, n_Q + n_D - 1]$ . If  $n_Q + n_D - 1 \geq 4$  we are done. Otherwise, by Property O2 of Lemma 3, we can optimally increase the spirality of  $G_\mu$  by inserting bends into the Q-nodes of  $\text{skel}(\mu)$ . Since  $n_Q \geq 2$  and the needed extra bends are at most three (because  $k \leq 4$ ), if we evenly distribute the extra bends among the real edges of  $\text{skel}(\mu)$ , we end up with at most two bends per edge, satisfying Property O1 of Lemma 3.  $\square$

**Candidate Representations for an R-node.** If  $\mu$  is an R-node, its children are S- or Q-nodes (Property T2 of Lemma 1). To compute a bend-minimum orthogonal representation of  $G_\mu$  that satisfies Properties O1–O3, we devise a variant of the linear-time algorithm by Rahman, Nakano, and Nishizeki [21] that exploits the properties of inner S-components.

**Lemma 8.** *Let  $\mu$  be an inner R-node and  $n_\mu$  be the number of vertices of  $\text{skel}(\mu)$ . There exists an  $O(n_\mu)$ -time algorithm that computes a set of candidate orthogonal representations of  $G_\mu$  such that every element of the set has at most two bends per edge.*

*Proof.* We first briefly recall the algorithm in [21], which we refer to as **MinBendCubic-Alg** and which is conceptually similar to **NoBend-Alg** (described in the proof of Lemma 3). **MinBendCubic-Alg** takes as input an embedded planar triconnected cubic graph  $\hat{G}$  and computes an embedding-preserving bend-minimum orthogonal representation of  $\hat{G}$ . It initially inserts four dummy vertices  $x, y, w, z$  of degree two on  $C_o(\hat{G})$ , by suitably subdividing some external edges; these vertices act as the four designated vertices of **NoBend-Alg**. Note that, since  $\hat{G}$  is triconnected, each maximal bad cycle  $C$  with respect to  $x, y, w, z$  is a 3-legged cycle. For each such cycle  $C$ , the algorithm collapses  $\hat{G}(C)$  into a supernode  $v_C$ , thus obtaining a coarser graph, which admits a rectangular representation  $R$  [27]. In the successive steps, for each supernode  $v_C$ , **MinBendCubic-Alg** recursively applies the same approach to compute an orthogonal representation of  $\hat{G}(C)$ , where three of the four designated vertices coincide with the leg-vertices of  $C$ . The representation of  $\hat{G}(C)$  is then plugged into  $R$ . All designated vertices added throughout the algorithm are bends of the final representation. Crucial to the bend-minimization process of **MinBendCubic-Alg** is the insertion of the designated vertices along edges that are shared by more than one bad cycles (if any). For example, let  $C_1$  and  $C_2$  be two bad cycles such

that  $C_1$  is maximal,  $C_2$  belongs to  $\hat{G}(C_1)$ , and  $C_1$  and  $C_2$  share a path  $p$ ; since both  $C_1$  and  $C_2$  need a bend, **MinBendCubic-Alg** inserts a designated vertex along  $p$  to save bends. At any step of the recursion, a *red* edge is an edge for which placing a designated vertex along it leads to a sub-optimal solution; the remaining edges are *green*. As it is proven in [21], every bad cycle has at least one green edge. A bad cycle  $C$  is a *corner cycle* if it has at least one green edge on the external face and there is no other bad cycle inside  $C$  having this property. In order to save bends when placing the four designated vertices on  $C_o(\hat{G})$ , **MinBendCubic-Alg** gives preference to the green edges of the corner cycles, if they exist. We remark that, algorithm **MinBendCubic-Alg** produces orthogonal drawings with at most one bend per edge, with the possible exception of one edge in the outer face, which is bent twice if the external boundary is a 3-cycle.

We now describe our algorithm, called **Rset-Alg**. Let  $\{u, v\}$  be the poles of  $\mu$ . **Rset-Alg** consists of two steps. In the first step it computes an  $\square$ -shaped orthogonal representation  $\hat{H}_\mu^\square$  and a  $\square$ -shaped orthogonal representation  $\tilde{H}_\mu^\square$  of  $\tilde{G}_\mu = \text{skel}(\mu) \setminus (u, v)$ , using a variant of **MinBendCubic-Alg**. In the second step, a bend-minimum  $\square$ -shaped orthogonal representation  $H_\mu^\square$  and a bend-minimum  $\square$ -shaped orthogonal representation  $\tilde{H}_\mu^\square$  of  $G_\mu$  are constructed, by replacing each virtual edge  $e_S$  in each of  $\hat{H}_\mu^\square$  and  $\tilde{H}_\mu^\square$  with the representation in the set of the corresponding S-node whose spirality equals the number of bends of  $e_S$ . Every time the algorithm needs to insert a designated vertex that subdivides an edge of the graph (either to break a bad cycle or to guarantee four external corners in the initial step), it adds this vertex on a virtual edge, if such an edge exists. Indeed, by Corollary 1, this vertex does not cause an additional bend in the final representation when the virtual edge is replaced by the corresponding S-component.

To find  $\tilde{H}_\mu^\square$ , where  $u$  and  $v$  are two of the four designated vertices on the external face of  $\tilde{G}_\mu$ , **Rset-Alg** has to find a further designated vertex on each of the two contour paths  $p_l$  and  $p_r$  of  $\tilde{G}_\mu$  from  $u$  to  $v$ . To do this, **Rset-Alg** first computes the corner cycles as in **MinBendCubic-Alg**, assuming that  $u$  and  $v$  are vertices of degree three, that is, attached with an additional leg to the rest of the graph. Since  $\text{skel}(\mu) = \tilde{G}_\mu \cup (u, v)$  is cubic and triconnected, the set of corner cycles computed in this way equals the set of corner cycles computed on  $\text{skel}(\mu)$ , for any of its two possible planar embeddings, minus those that involve  $(u, v)$ , if any. Edges on each of the two contour paths  $p \in \{p_l, p_r\}$  are classified as follows: a virtual edge of a corner cycle is *free- $\mathcal{E}$ -useful* ('free' because a bend on such an edge does not correspond to a bend in the final orthogonal representation; 'useful' because it also satisfies condition (iii) of Theorem 2 for some 3-legged cycle); a virtual edge that does not belong to a corner cycle is *free- $\mathcal{E}$ -useless*; a (real) edge of a corner cycle is *costly- $\mathcal{E}$ -useful* ('costly' because a bend on such edge is an actual bend in the final orthogonal representation); any other real edge is *costly- $\mathcal{E}$ -useless*. Note that if the edge  $e_l$  of  $p_l$  incident to  $u$  (resp.  $v$ ) is useful, also the edge  $e_r$  of  $p_r$  incident to  $u$  (resp.  $v$ ) is useful. However, choosing one between  $e_l$  and  $e_r$  is enough to satisfy condition (iii) of Theorem 2 for their common 3-legged cycles. Hence, choosing  $e_l$  will transform  $e_r$  into a useless edge and vice versa. The two designated vertices on  $p_l$  and  $p_r$  are chosen in such a way to minimize the sum of the number of useless and the number of the costly edges, which implies the minimization of the number of bends introduced in the final orthogonal drawing of  $G_\mu$ . Once the four designated vertices are chosen, **Rset-Alg** proceeds recursively as **MinBendCubic-Alg**. However, each time a new designated vertex has to be added to break a bad cycle  $C$ , the edge of  $C$  along which this vertex is added is chosen according to the following priority: (i) a virtual green edge; (ii) a virtual red edge; (iii) a (real) green edge; (iv) any other real edge.

The computation of  $\tilde{H}_\mu^\square$  is similar to that of  $\hat{H}_\mu^\square$ , with the difference that the two designated vertices on the external face of  $\tilde{G}_\mu$ , in addition to  $u$  and  $v$ , must be inserted both on  $p_l$  or both on  $p_r$ . Further, if a virtual edge  $e_{\mu'}$  on the external face of  $\tilde{G}_\mu$  corresponds to a child  $\mu'$  of  $\mu$  that admits an orthogonal drawing with spirality two at the same cost of the orthogonal drawing with spirality zero, then we call such an edge *double-free*, since it can host both the designated vertices without additional costs, and allow it to be chosen two times (only one of the two choices can be useful). Two different computations are performed, one for each contour path, and only the cheapest in terms of bends is considered.

Concerning the time complexity, **Rset-Alg** can be implemented to run in  $O(n_\mu)$ . Indeed, the first step of **Rset-Alg** is a simple modification of **MinBendCubic-Alg**, and thus it works in  $O(n_\mu)$  time. The orthogonal representations  $\hat{H}_\mu^\square$  and  $\tilde{H}_\mu^\square$  are then described in a succinct way, by linking the desired representations of the S-component for each virtual edge.  $\square$

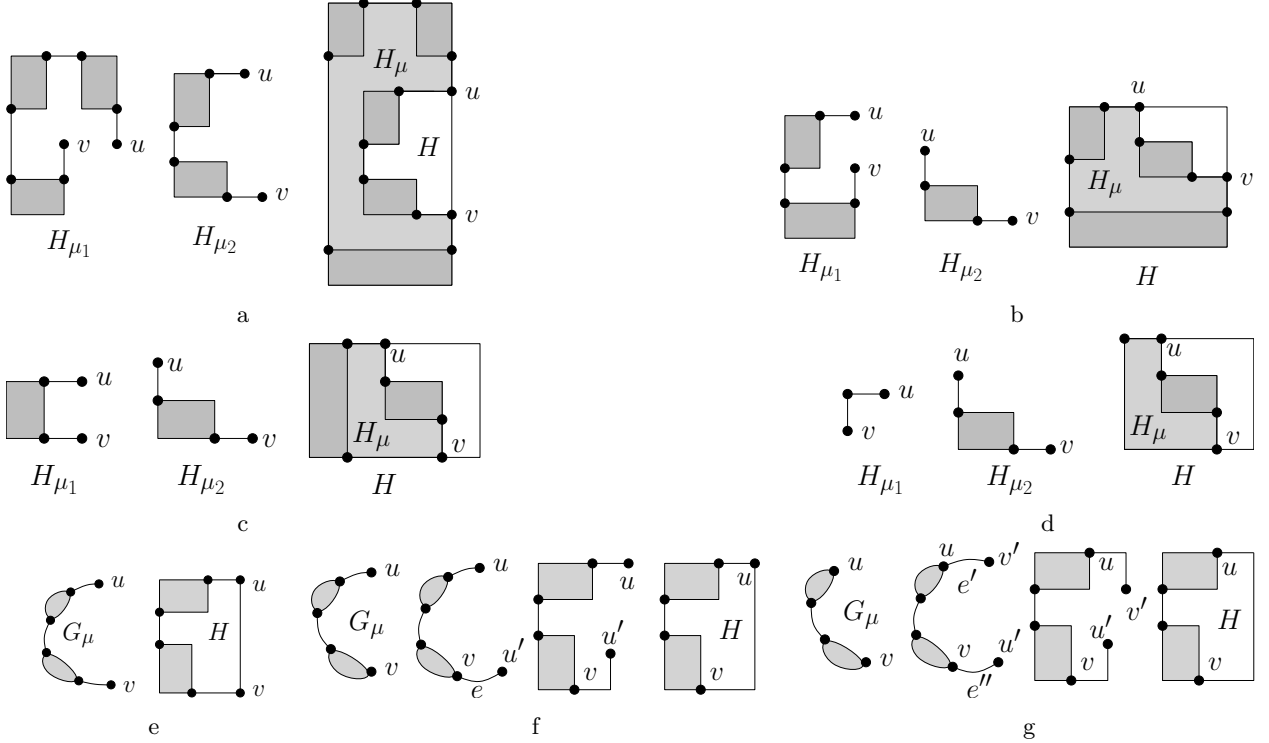


Figure 6: Examples of: (a)-(d) a P-node root child; (e)-(f) an S-node root child.

## 4.2 Handling the root child component

Let  $T$  be the SPQR-tree of  $G$  with respect to edge  $e = (u, v)$  and let  $\mu$  be the root child of  $T$ . Assuming to have already computed the set of candidate representations for the children of  $\mu$ , we compute an orthogonal representation  $H_\mu$  of  $G_\mu$  and a bend-minimum orthogonal representation  $H$  of  $G$  (with  $e$  on the external face) depending on the type of  $\mu$ .

**Algorithm P-root-child.** Let  $\mu$  be a P-node and let  $\mu_1$  and  $\mu_2$  be its children. By Property T1 of Lemma 1 and since  $G$  is simple, both  $\mu_1$  and  $\mu_2$  are S-nodes. Let  $k_1$  (resp.  $k_2$ ) be the maximum spirality of a representation  $H_{\mu_1}$  (resp.  $H_{\mu_2}$ ) at the same cost  $c_{0,1}$  (resp.  $c_{0,2}$ ) of a representation with spirality 0. Assume, w.l.o.g., that  $k_1 \geq k_2$ . We have three cases:

Case 1:  $k_1 \geq 4$ . Get a  $\boxtimes$ -shaped  $H_\mu$  by merging a representation of  $\mu_1$  with spirality 4 and one of  $\mu_2$  with spirality 2.  $H$  is obtained adding  $e$  with 0 bends (Fig. 6a).

Case 2:  $k_1 = 3$ . Get an  $\boxplus$ -shaped  $H_\mu$  by merging a representation of  $\mu_1$  with spirality 3 and one of  $\mu_2$  with spirality 1.  $H$  is obtained adding  $e$  with 1 bend (Fig. 6b).

Case 3:  $k_1 = 2$  or  $k_2 = k_1 = 1$ . Get a  $\boxdot$ -shaped  $H_\mu$  by merging a representation of  $\mu_1$  with spirality 2 and one of  $\mu_2$  with spirality 0.  $H$  is obtained adding  $e$  with 2 bends (Figs. 6c- 6d).

**Lemma 9.** *Algorithm P-root-child computes a bend-minimum orthogonal representation of  $G$  with  $e$  on the external face and at most two bends per edge in  $O(1)$  time.*

*Proof.* Observe that any orthogonal representation of  $\mu$  satisfies the property that the spirality of  $\mu_1$  plus the number of bends of the edge  $(u, v)$  is at least four. This property, that we call the *cycle-property*, is due to the fact that  $\mu_1$  and  $(u, v)$  have to close a cycle containing the drawing of  $\mu_2$ . Further, since by hypothesis  $c_{0,1}$  and  $c_{0,2}$  are the minimum number of bends for an orthogonal drawing of  $G_{\mu_1}$  and  $G_{\mu_2}$ , respectively,  $G$  does not admit an orthogonal representation with fewer than  $c_{0,1} + c_{0,2}$  bends. We consider the costs

of the solutions in the four different cases. **Case 1:** the cost is  $c_{0,1} + c_{0,2}$  if  $k_2 \geq 2$ , which is the minimum possible. Otherwise, by Corollary 1 we have  $k_2 = 1$  and the cost is  $c_{0,1} + c_{0,2} + 1$ . This is again the minimum, because drawing  $\mu_2$  with spirality 1 would save a bend for  $\mu_2$ , but would force  $(u, v)$  to have one bend. **Case 2:** the cost is  $c_{0,1} + c_{0,2} + 1$ , which is the minimum since the cycle-property forces one between  $\mu_1$  or  $(u, v)$  to host a bend. The same consideration proves that the cost is minimum also for case **Case 3**, where the costs are  $c_{0,1} + c_{0,2} + 2$  and  $c_{0,1} + c_{0,2} + 3$ , respectively. The obtained orthogonal representation trivially satisfies Properties O1–O3, since they are satisfied by hypothesis by the candidate representations of  $\mu_1$  and  $\mu_2$  and  $(u, v)$  has at maximum two bends.  $\square$

**Algorithm S-root-child.** Let  $\mu$  be an S-node. if  $G_\mu$  starts and ends with one edge, then we compute the candidate orthogonal representations of  $G_\mu$  as if it were an inner S-node, and we obtain  $H$  by adding  $e$  with zero bends to the representation of  $G_\mu$  with spirality 2 (Fig. 6e). Else, if  $G_\mu$  only starts or ends with one edge, then we add  $e$  to the other end of  $G_\mu$ , we compute the candidate representations of  $G_\mu \cup \{e\}$  as if it were an inner S-node, and we obtain  $H$  by adopting the representation of  $G_\mu \cup \{e\}$  with spirality 3 and by identifying the first and last vertex (Fig. 6f). Finally, if  $\text{skel}(\mu) \setminus \{e\}$  starts and ends with a Q-node or a P-node, we add two copies  $e'$  and  $e''$  of  $e$  at the beginning and at the end of  $G_\mu$ , we compute the candidate representations of  $G_\mu \cup \{e', e''\}$  as if it were an inner S-node, and we obtain  $H$  by adopting the representation of  $G_\mu \cup \{e', e''\}$  with spirality 4, by identifying the first and last vertex of  $G_\mu \cup \{e', e''\}$  and by smoothing the resulting vertex (Fig. 6g).

**Lemma 10.** *Algorithm S-root-child computes a bend-minimum orthogonal representation of  $G$  with  $e$  on the external face and at most two bends per edge in  $O(n_\mu)$  time, where  $n_\mu$  be the number of vertices of  $\text{skel}(\mu)$ .*

*Proof.* The fact that the number of bends is minimum descends from the evidence that it is always convenient to increase the spirality of a series, as it only costs one unit for each unit of increased spirality (Lemma 6). The obtained orthogonal representation satisfies Properties O1–O3. In fact, no edge receives more than two bends. In the first case  $(u, v)$  is added without bends. In the second case,  $G_\mu \cup \{e\}$  is a series with at least two Q-nodes (including  $e$ ), which guarantees that it admits an orthogonal drawing with spirality 1 without bending the Q-nodes and of spirality three with at most two bends on such Q-nodes. In the third case,  $G_\mu \cup \{e', e''\}$  is a series with at least three Q-nodes (including  $e'$  and  $e''$ ). Hence, an orthogonal drawing with spirality 4 has at most two bends on these Q-nodes.  $\square$

**Algorithm R-root-child.** Let  $\mu$  be an R-node. Consider the two planar embeddings  $\phi_1$  and  $\phi_2$  of  $\text{skel}(\mu)$  obtained by choosing as external face one of the two faces incident to  $e$ . For each  $\phi_i$ , we compute an orthogonal representation  $H_i$  of  $G$  by: (i) Finding a representation  $\tilde{H}_i$  on the entire  $\text{skel}(\mu)$  (included  $e$ ) with the same variant of [21] described in the proof of Lemma 8, but this time assuming that all four designated corners of the external face in the initial step must be found; (ii) Replacing each virtual edge that bends  $k \geq 0$  times in  $\tilde{H}_i$  with a minimum-bend representation of its corresponding S-component with spirality  $k$ .  $H$  is the cheapest of  $H_1$  and  $H_2$ . Since the variant of [21] applied to  $\text{skel}(\mu)$  still causes at most two bends per edge, with the same arguments as in Lemma 8 we have:

**Lemma 11.** *Algorithm R-root-child computes a bend-minimum orthogonal representation of  $G$  with  $e$  on the external face and at most two bends per edge in  $O(n_\mu)$  time, where  $n_\mu$  be the number of vertices of  $\text{skel}(\mu)$ .*

### 4.3 Simply-Connected Graphs and Proof of Theorem 1

We exploit the block-cut-vertex tree (or BC-tree)  $\mathcal{T}$  of the simply-connected 3-planar graph  $G$ , where each node of  $\mathcal{T}$  is either a block or a cut-vertex and cut-vertices are adjacent to the blocks they belong to. Call *trivial blocks* those composed of a single edge and *full blocks* the remaining. Since  $\Delta(G) \leq 3$ , full blocks are only adjacent to trivial blocks. Also, cut-vertices of degree three are adjacent to three trivial blocks. All trivial blocks admit a drawing with zero bends as straight edges. Let  $e$  be an edge that is chosen to be on the external face. Root  $\mathcal{T}$  at the block  $B_e$  containing  $e$  and compute in  $O(n_e)$  time, where  $n_e$  is the number of vertices of  $B_e$ , a bend-minimum orthogonal representation  $H_e$  of  $B_e$  with  $e$  on the external face as described

in Sections 4.1 and 4.2. Build an optimal orthogonal representation  $H$  of  $G$  by recursively attaching pieces to the initial orthogonal representation  $H_e$ . Let  $v$  be a cut-vertex of the current orthogonal representation  $H$  and let  $B_v$  a child block attached to  $v$ . Compute an optimal orthogonal representation  $H_v$  of  $B_v$  with  $v$  on the external face and attach it to  $v$ . Since  $\deg(v) \leq 2$  in  $B_v$ , in order to have  $v$  on the external face it suffices to have one of its two incident edges on the external face. Hence, the required orthogonal representation  $H_v$  can be computed in  $O(n_v)$  time, where  $n_v$  is the number of vertices of  $B_v$ .

**Proof of Theorem 1.** For a distinguished edge  $e$  of  $G$ , Lemmas 5, 7, 8 and Lemmas 9–11 yield an  $O(n)$ -time algorithm that computes a bend-minimum orthogonal representation of  $G$  with  $e$  on the external face and with at most two bends per edge. Call **BendMin-RefEdge** this algorithm. Running **BendMin-RefEdge** for every possible choice of the reference edge, we find in  $O(n^2)$  time a bend-minimum orthogonal representation of  $G$  over all its planar embeddings. If  $v$  is a distinguished vertex of  $G$ , running **BendMin-RefEdge** for every edge incident to  $v$ , we find in  $O(n)$  time a bend-minimum orthogonal representation of  $G$  with  $v$  on the external face (recall that  $\deg(v) \leq 3$ ). Finally, recall that an orthogonal drawing of  $G$  can be computed in linear-time from an orthogonal representation of  $G$  [7].

## 5 Conclusions and Open Problems

We described the first  $O(n^2)$ -time algorithm to compute a bend-minimum orthogonal drawing of a planar 3-graph in the variable embedding setting. If a distinguished edge or vertex is constrained to be on the external face our technique works in  $O(n)$ -time. Our results are proved by means of a non-flow based approach, which is the main difference between our paper and previous work on the same problem [4, 8]. A non-flow based algorithm having some similarities with ours is described in [12], which however does not compute bend-minimum drawings. We conclude by listing two research directions related to our results.

- (a) It would be interesting to design other linear-time algorithms for bend-minimum orthogonal drawings of planar 3-graphs in the variable embedding setting. For example, is there a linear-time algorithm to compute a bend-minimum orthogonal drawing of a triconnected planar cubic graph, for every possible choice of the external face?
- (b) The question about whether a linear-time algorithm for the bend-minimization problem in the fixed embedding setting exists is still open [14]. It is interesting to study this problem by means of non-flow based approaches. In this direction, a positive answer is given in [22] for the case of plane 3-graphs.

## References

- [1] T. C. Biedl and G. Kant. A better heuristic for orthogonal graph drawings. *Comput. Geom.*, 9(3):159–180, 1998.
- [2] T. Bläsius, I. Rutter, and D. Wagner. Optimal orthogonal graph drawing with convex bend costs. *ACM Trans. Algorithms*, 12(3):33:1–33:32, 2016.
- [3] F. Brandenburg, D. Eppstein, M. T. Goodrich, S. G. Kobourov, G. Liotta, and P. Mutzel. Selected open problems in graph drawing. In G. Liotta, editor, *Graph Drawing, 11th International Symposium, GD 2003, Perugia, Italy, September 21-24, 2003, Revised Papers*, volume 2912 of *Lecture Notes in Computer Science*, pages 515–539. Springer, 2003.
- [4] Y. Chang and H. Yen. On bend-minimized orthogonal drawings of planar 3-graphs. In B. Aronov and M. J. Katz, editors, *33rd International Symposium on Computational Geometry, SoCG 2017, July 4-7, 2017, Brisbane, Australia*, volume 77 of *LIPICS*, pages 29:1–29:15. Schloss Dagstuhl - Leibniz-Zentrum fuer Informatik, 2017.
- [5] M. B. Cohen, A. Madry, D. Tsipras, and A. Vladu. Matrix scaling and balancing via box constrained newton’s method and interior point methods. In C. Umans, editor, *58th IEEE Annual Symposium on Foundations of Computer Science, FOCS 2017, Berkeley, CA, USA, October 15-17, 2017*, pages 902–913. IEEE Computer Society, 2017.
- [6] S. Cornelsen and A. Karrenbauer. Accelerated bend minimization. *J. Graph Algorithms Appl.*, 16(3):635–650, 2012.
- [7] G. Di Battista, P. Eades, R. Tamassia, and I. G. Tollis. *Graph Drawing: Algorithms for the Visualization of Graphs*. Prentice-Hall, 1999.
- [8] G. Di Battista, G. Liotta, and F. Vargiu. Spirality and optimal orthogonal drawings. *SIAM J. Comput.*, 27(6):1764–1811, 1998.
- [9] W. Didimo and G. Liotta. Mining graph data. In D. J. Cook and L. B. Holder, editors, *Graph Visualization and Data Mining*, pages 35–64. Wiley, 2007.
- [10] W. Didimo, G. Liotta, and M. Patrignani. On the complexity of HV-rectilinear planarity testing. In C. Duncan and A. Symvonis, editors, *Proc. 22nd International Symposium on Graph Drawing (GD ’14)*, volume 8871 of *Lecture Notes in Computer Science*, pages 343–354, 2014.
- [11] C. A. Duncan and M. T. Goodrich. Planar orthogonal and polyline drawing algorithms. In R. Tamassia, editor, *Handbook on Graph Drawing and Visualization.*, pages 223–246. Chapman and Hall/CRC, 2013.
- [12] A. Garg and G. Liotta. Almost bend-optimal planar orthogonal drawings of biconnected degree-3 planar graphs in quadratic time. In J. Kratochvíl, editor, *Graph Drawing, 7th International Symposium, GD’99, Stirín Castle, Czech Republic, September 1999, Proceedings*, volume 1731 of *Lecture Notes in Computer Science*, pages 38–48. Springer, 1999.
- [13] A. Garg and R. Tamassia. On the computational complexity of upward and rectilinear planarity testing. *SIAM J. Comput.*, 31(2):601–625, 2001.
- [14] E. D. Giacomo, G. Liotta, and R. Tamassia. Graph drawing. In J. Goodman, J. O’Rourke, and C. Toth, editors, *Handbook of Discrete and Computational Geometry, Third Edition*, pages 1451–1477. Chapman and Hall/CRC, 2017.
- [15] C. Gutwenger and P. Mutzel. A linear time implementation of spqr-trees. In J. Marks, editor, *Graph Drawing, 8th International Symposium, GD 2000, Colonial Williamsburg, VA, USA, September 20-23, 2000, Proceedings*, volume 1984 of *Lecture Notes in Computer Science*, pages 77–90. Springer, 2000.

- [16] J. E. Hopcroft and R. E. Tarjan. Dividing a graph into triconnected components. *SIAM J. Comput.*, 2(3):135–158, 1973.
- [17] M. Jünger and P. Mutzel, editors. *Graph Drawing Software*. Springer, 2004.
- [18] M. Kaufmann and D. Wagner, editors. *Drawing Graphs, Methods and Models (the book grow out of a Dagstuhl Seminar, April 1999)*, volume 2025 of *Lecture Notes in Computer Science*. Springer, 2001.
- [19] Y. Liu, A. Morgana, and B. Simeone. A linear algorithm for 2-bend embeddings of planar graphs in the two-dimensional grid. *Discrete Applied Mathematics*, 81(1-3):69–91, 1998.
- [20] T. Nishizeki and M. S. Rahman. *Planar Graph Drawing*, volume 12 of *Lecture Notes Series on Computing*. World Scientific, 2004.
- [21] M. S. Rahman, S. Nakano, and T. Nishizeki. A linear algorithm for bend-optimal orthogonal drawings of triconnected cubic plane graphs. *J. Graph Algorithms Appl.*, 3(4):31–62, 1999.
- [22] M. S. Rahman and T. Nishizeki. Bend-minimum orthogonal drawings of plane 3-graphs. In L. Kucera, editor, *Graph-Theoretic Concepts in Computer Science, 28th International Workshop, WG 2002, Cesky Krumlov, Czech Republic, June 13-15, 2002, Revised Papers*, volume 2573 of *Lecture Notes in Computer Science*, pages 367–378. Springer, 2002.
- [23] M. S. Rahman, T. Nishizeki, and M. Naznin. Orthogonal drawings of plane graphs without bends. *J. Graph Algorithms Appl.*, 7(4):335–362, 2003.
- [24] J. A. Storer. The node cost measure for embedding graphs on the planar grid (extended abstract). In R. E. Miller, S. Ginsburg, W. A. Burkhard, and R. J. Lipton, editors, *Proceedings of the 12th Annual ACM Symposium on Theory of Computing, April 28-30, 1980, Los Angeles, California, USA*, pages 201–210. ACM, 1980.
- [25] R. Tamassia. On embedding a graph in the grid with the minimum number of bends. *SIAM J. Comput.*, 16(3):421–444, 1987.
- [26] R. Tamassia, I. G. Tollis, and J. S. Vitter. Lower bounds for planar orthogonal drawings of graphs. *Inf. Process. Lett.*, 39(1):35–40, 1991.
- [27] C. Thomassen. Plane representations of graphs. In J. Bondy and U. Murty, editors, *Progress in Graph Theory*, pages 43–69. 1987.
- [28] G. Vijayan and A. Wigderson. Rectilinear graphs and their embeddings. *SIAM Journal on Computing*, 14(2):355–372, 1985.
- [29] X. Zhou and T. Nishizeki. Orthogonal drawings of series-parallel graphs with minimum bends. *SIAM J. Discrete Math.*, 22(4):1570–1604, 2008.